

Pegylated and Thermosensitive Polyion Complex Micelles by Self-Assembly of Two Oppositely and Permanently Charged Diblock Copolymers

Serena De Santis,[†] Rita Diana Ladogana,[†] Marco Diociaiuti,[‡] and Giancarlo Masci^{*,†}

[†]Department of Chemistry, University of Rome “La Sapienza”, P. le A. Moro 5, 00185 Rome, Italy, and

[‡]Dipartimento di Tecnologie e Salute, Istituto Superiore di Sanità, Viale R. Elena 299, 00161, Roma, Italy

Received December 1, 2009; Revised Manuscript Received January 12, 2010

ABSTRACT: Thermosensitive and pegylated polyion complex (PIC) micelles were formed by coassembly of oppositely and permanently charged poly(sodium 2-acrylamido-2-methylpropanesulfonate)-*block*-poly(*N*-isopropylacrylamide), PAMPS-*b*-PNIPAAm, and poly[(3-acrylamidopropyl)-trimethylammonium chloride]-*block*-poly(ethylene oxide), PAMPTMA-*b*-PEO, block copolymers under stoichiometric charge neutralization conditions and polyelectrolyte chain length matching. PAMPTMA-*b*-PEO block copolymers with different block lengths were prepared for the first time by atom transfer radical polymerization (ATRP) using a PEO macroinitiator. PIC micelles were characterized by ¹H NMR, static light scattering (SLS), dynamic light scattering (DLS), and transmission electron microscopy (TEM). At room temperature, spherical almost monodisperse PIC micelles, consisting of a mixed PAMPTMA/PAMPS coacervate core and a mixed PEO/PNIPAAm shell, were formed, with size of about 80–110 nm. The PIC micelles completely dissociated to unimers by increasing NaCl concentration above 0.4–0.6 M. PNIPAAm segments in the shell gave rise to a temperature induced transition at 34–37 °C forming a hydrophobic shell around the coacervate core in a core–shell–corona type PIC micelle, with a PEO corona which stabilized the nanoparticles in aqueous solution. A fully interconnected and continuous collapsed PNIPAAm shell was formed, with PEO chains forming channels across the PNIPAAm membrane. The association properties of the PIC micelles were influenced by the length of the block segments. Longer polyelectrolyte chains gave rise to bigger micelles, more stable with respect to the ionic strength. PNIPAAm chain length allowed to modulate the temperature of the thermal transition. Long PEO chains (114 repeating units) were necessary to effectively stabilize PIC micelles both below and above LCST of PNIPAAm. Micelle parameters (core radius, R_c , shell radius, R_s , thickness and volume, $\Delta R_{PNIPAAm}$ and $V_{PNIPAAm}$, of the collapsed PNIPAAm shell and surface density, Φ , of shell and corona chains before and after the thermal transition) were determined and discussed in terms of block copolymer structure. Precipitation was observed by addition of salt at temperature above LCST because of the release of PEO-*b*-PAMPTMA chains. A model was proposed explaining the formation and the response to temperature and ionic strength of the PIC micelles. This is the first example of pegylated and thermosensitive PIC micelles having a coacervate core formed by two strong polyelectrolyte blocks with no pH dependence.

Introduction

Generally, polymer-based nanostructured materials such as micelles and vesicles have been prepared by self-association of block copolymers driven by noncovalent interactions including hydrogen bonding and van der Waals, hydrophobic, and electrostatic interactions. Even though hydrophobic self-association has been the most widely used up to now, more attention has been gained recently by the so-called polyion complex (PIC) micelles formed by coassembly of oppositely charged polymers and block copolymers.^{1–20} In most cases, at least one block copolymer contains a charged segment and a water-soluble uncharged segment made of poly(ethylene oxide), PEO, which stabilizes PIC micelles surrounding the interpolyelectrolyte coacervate core. Another advantage of using PEO, if PIC are designed for biomedical application, is its well-known biocompatibility and antifouling activity to proteins,^{21–23} platelets^{24,25} and cells.^{24,26,27} Kataoka and Harada were the first to report on PIC micelles with narrow size distribution prepared by coassembly of oppositely

charged block copolymers made of charged poly(amino acid) and PEO.^{9,13,15–17} Recently kataoka et al. have also demonstrated that PIC micelles prepared starting from block copolymers of PEO, poly(α,β -aspartic acid) and poly([*N*-(2-aminoethyl)-2-aminoethyl]- α,β -aspartamide) in which the blocks are linked by cleavable disulfide bonds can be used as template for the formation of biocompatible nanocapsules.²⁸

Recent development in living free radical polymerization methods allowed the syntheses of various amphiphilic block copolymers with controlled structure that can self-assemble in aqueous solution.²⁹ These methods have also been used to synthesize oppositely charged block copolymers, poly[sodium 2-(acrylamido)-2-methylpropanesulfonate]-*block*-poly(ethylene oxide), PAMPS-*b*-PEO, and poly[3-(methacryloylamino)propyl]trimethylammonium chloride]-*block*-poly(ethylene oxide), PMAPTAC-*b*-PEO, that were used to prepare pegylated PIC micelles.¹

Stimulus responsive hydrophilic polymers are an interesting class of polymers that by a proper stimulus such as temperature, pH, or ionic strengths, can become insoluble in water. One of the most interesting “sensitive” polymer is poly(*N*-isopropylacrylamide) (PNIPAAm), a thermoresponsive polymer which

*Corresponding author. E-mail: giancarlo.masci@uniroma1.it. Telephone: +39-06-49913677.

is water-soluble at room temperature and is able to give a coil-to-globule transition above its lower critical solution temperature (LCST) of 32 °C.^{30,31} PNIPAA copolymers have attracted a lot of attention as the LCST in water is close to body temperature and may thus be useful in the biomedical field as a stimulus-sensitive material. Two examples of PNIPAA functionalized PIC micelles have been reported in the literature.^{10,12} Voets et al. prepared thermosensitive PIC micelles by coassembly in aqueous solution at room temperature of poly(*N*-methyl-2-vinylpyridinium iodide)-*block*-poly(ethylene oxide), P2MVP-*b*-PEO and poly(acrylic acid)-*block*-poly(*N*-isopropylacrylamide), PAA-*b*-PNIPAA.¹⁰ These PIC micelles, with a coacervate core of PAA and P2MVP surrounded by a corona of PNIPAA and PEO chains at room temperature, showed temperature responsiveness, rearranging and forming an “onion” or “core-shell-corona” structure above LCST. Li et al. prepared thermosensitive PIC micelles by self-assembling a heteroarm star polymer, poly(ethylene oxide)-poly(*N*-isopropylacrylamide)-poly(L-lysine), PEO-PNIPAAm-PLys, with oppositely charged poly(acrylic acid), PAA.¹²

Other authors prepared similar self-assembled core-shell thermosensitive nanoparticles formed by a hydrophobic core instead of a coacervate core, surrounded by a shell made of PNIPAAm and another hydrophilic polymer. Shi et al. prepared complex micelles formed by a poly(4-vinylpyridine), P4VP, core and a shell of PEO and PNIPAAm.³² In another paper, Shi et al. prepared complex micelles with a poly(*tert*-butyl acrylate), PtBA, core surrounded by a shell of PNIPAAm and protonated P4VP.³³

Here we report the first example of formation of PIC micelles with a thermosensitive and antifouling shell starting from two block copolymers having oppositely charged blocks with no dependence on pH. The block copolymers used in this study are poly(ethylene oxide)-*block*-poly[(3-acrylamidopropyl)-trimethylammonium chloride], PEO-*b*-PAMPTMA, containing a quaternized polyacrylamide cationic block and PAMPS-*b*-PNIPAAm, containing a strong acid sulfonate polyacrylamide anionic block. Hence, both block copolymers have a degree of ionization independent of pH. PAMPS-*b*-PNIPAAm ATRP synthesis has been already reported by our group.³⁴ ATRP synthesis of PEO-*b*-PAMPTMA block copolymers will be described in this manuscript. PIC micelles formed by mixing block copolymers with different block length will be characterized by ¹H NMR spectroscopy, transmission electron microscopy (TEM), and dynamic and static light scattering (DLS, SLS) as a function of block copolymer composition, ionic strength, and temperature. The PIC micelles parameters will be discussed in terms of the above-mentioned variables and a model describing PIC micelles formation, thermosensitivity, and ionic strength dependence will be proposed.

Experimental Section

Materials. Tris(2-dimethylaminoethyl)amine (Me₆TREN) was synthesized as previously described.³⁵ Poly(ethylene oxide) methyl ether with average molecular weight ~2000 (PEO₄₅-OH, $M_w/M_n = 1.04$) and 5000 (PEO₁₁₄-OH, $M_w/M_n = 1.03$) from Aldrich were used as received without further purification. CuCl from Fluka was washed with acetic acid followed by methanol to remove impurities. CuCl₂ from Fluka was used as received. (3-acrylamidopropyl)-trimethylammonium chloride (AMPTMA, 75% w/v in water, $d = 1.12$ g/mL) from Aldrich was used as received. *N*-Isopropylacrylamide (NIPAAm, Aldrich) was recrystallized from hexane and dried under vacuum prior to use. Ethyl 2-chloropropionate (ECP, Aldrich) and all other reagents were used as received.

Synthesis of Poly(ethylene oxide)-Based Macroinitiators (PEO₄₅-Br and PEO₁₁₄-Br). In a three-neck flask under argon

atmosphere, PEO-OH was dissolved in toluene. Traces of water were removed by Soxhlet extraction with molecular sieves (4 Å) for 4 h. Triethylamine was added, and the solution was cooled to 0 °C. 2-Bromopropionyl bromide (1.5 molar equiv with respect to PEO) was added dropwise via a dropping funnel over 30 min, and the reaction mixture was stirred overnight at room temperature. The solution was filtered to remove the triethylamine hydrochloride precipitate and most of the toluene was removed by rotary evaporation prior to precipitation of the polymer in a 10-fold excess of ethyl ether. The crude polymer was repeatedly washed with ethyl ether and dried under vacuum to yield the purified macroinitiator.

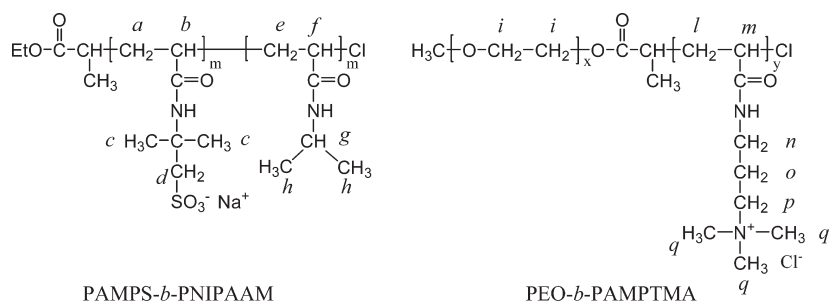
Preparation of Cationic Diblock Copolymers (PEO-*b*-PAMPTMA). As an example, for the preparation of the diblock copolymer PEO₁₁₄-*b*-PAMPTMA₁₀₀ we used DMF:water 50:50 (v/v), $T = 20$ °C, [AMPTMA]:[PEO-Br]:[CuCl]:[Me₆TREN] = 120:1:1:1 and [AMPTMA] = 1.25 M. AMPTMA (5.50 mL, 20.0 mmol), PEO-Br (0.858 g, 0.167 mmol of initiating groups), 3.5 mL of water and 8.0 mL of DMF were introduced in a Schlenk tube and degassed purging with argon. In a 25 mL, two-necked, round-bottomed flask previously degassed by three vacuum-argon cycles, a Cu(I)-Me₆TREN water stock solution was prepared adding 5 mL of degassed water to 133.4 mg (0.334 mmol) of CuCl and 84 μL (0.334 mmol) of Me₆TREN. After taking from the Schlenk tube an initial sample to measure the monomer concentration at $t = 0$, 2.5 mL of the freshly prepared Cu(I)-Me₆TREN water stock solution was added. The solution turned light green as the complex formation occurred. The polymerization was carried out at 20 °C. To measure the monomer conversion by HPLC, samples were withdrawn and diluted up in the eluent. At the same time, a given amount of reaction mixture was withdrawn and diluted in the GPC eluent for the molecular weight determination. At the end of the polymerization the mixture was diluted, bubbled with air for 5 min to stop the polymerization and extensively dialyzed against distilled water. The solid product was obtained by lyophilization. Three block copolymers with different length of PEO and PAMPTMA were prepared and will be named PEO₄₅-*b*-PAMPTMA₁₀₀, PEO₁₁₄-*b*-PAMPTMA₁₀₀, and PEO₁₁₄-*b*-PAMPTMA₅₀, with the subscript indicating the number-average degree of polymerization of the block.

Preparation of Anionic Thermosensitive Diblock Copolymers (PAMPS-*b*-PNIPAAm). The copolymers were prepared by preparation of a PAMPS macroinitiator and subsequent block copolymerization of this macroinitiator with PNIPAAm as already reported in our previous paper.³⁴ Three block copolymers were used: PAMPS₃₆-*b*-PNIPAAm₉₆, PAMPS₉₈-*b*-PNIPAAm₉₄, and PAMPS₉₈-*b*-PNIPAAm₄₀. M_n , M_w , and M_w/M_n data are reported elsewhere.³⁴ The PAMPS block was in the sodium form.

Preparation of Polyion Complex Micelles. PEO-*b*-PAMPTMA and PAMPS-*b*-PNIPAAm were separately dissolved in a 0.001 M NaCl aqueous solution that were allowed to stand overnight at room temperature to achieve complete dissolution. For the preparation of PIC micelles, a PEO-*b*-PAMPTMA solution (10 mg/mL) was quickly added to a PAMPS-*b*-PNIPAAm solution (1 mg/mL) at room temperature with vigorous stirring and the mixture was allowed to equilibrate until a stable scattered intensity was obtained. Finally the PIC concentration was adjusted at 1 mg/mL by adding 0.001 M NaCl. The mixing ratio of the two block copolymers was chosen to obtain complete charge neutralization. PIC will be named A_xN_y/E_nA_m, with A_xN_y and E_nA_m corresponding to PAMPS_x-*b*-PNIPAAm_y and PEO_n-*b*-PAMPTMA_m, respectively.

Characterization. ¹H NMR. ¹H NMR spectra were recorded at 298 and 323 K on a Varian XL-300 spectrometer operating at 300 MHz. Chemical shifts in D₂O were reported in ppm with respect to a trace of 2,2-dimethyl-2-silapentane-5-sulfonate sodium salt (DSS) used as an internal standard.

Scheme 1



The samples (~ 10 mg) were solubilized in D_2O (800 μL) and the spectra recorded at 398 K.

HPLC. HPLC experiments for the determination of monomer conversion were performed using a LabFlow 4000 HPLC pumps (LabService Analytica, Bologna, Italy) equipped with a Knauer K-2501 UV detector and a C18 (Phenomenex Luna, 5 μm) Column. AMPTMA was analyzed eluting with water/acetonitrile/acetic acid 90/5/5 (v/v/v). The injection volume was 10 μL . DMF was used as internal standard.

GPC. Molecular weight distributions were obtained using a GPC system equipped with a LabFlow 4000 HPLC pump, TSK-GEL α -3000 (30 cm \times 7.8 mm ID, 7 μm) column and a Shimadzu RID-10A refractive index detector (Shimadzu, Kyoto, Japan). The columns were thermostated at 40 $^{\circ}C$. PEO-*b*-PAMPTMA was eluted at a flow rate of 0.8 mL/min with 0.1 M Na_2SO_4 . The number-average molecular weight (M_n) and the molecular weight distribution (M_w/M_n) were determined by calibration with near-monodisperse poly(ethylene oxide) (PEO) standards. As PEO standards were not eluted with 0.1 M Na_2SO_4 and PEO-*b*-PAMPTMA was not eluted with water, the calibration was made eluting PEO with water containing 0.05% NaN_3 and then calculating PEO-*b*-PAMPTMA molecular weights with respect to this calibration curve using the lactose peak as elution time internal standard. The concentration of the polymeric solutions was 1 mg/mL. The injection volume was 50 μL .

Refractive Index Increment (dn/dc). dn/dc was measured at 25 $^{\circ}C$ with a refractive index detector (Δn -1000 RI, WGE Dr. Bures) working at 633 nm using the static method (see Supporting Information).

Dynamic Light Scattering (DLS). DLS data were obtained with a Brookhaven Instruments Corp. BI-200SM goniometer equipped with a BI-9000AT digital correlator using a solid-state laser (125 mW, $\lambda = 532$ nm). If not otherwise stated, measurements of scattered light were made at a scattering angle θ of 90 $^{\circ}$. The temperature of the copolymer solution was controlled with accuracy of 0.1 $^{\circ}C$. All samples were prepared by filtering about 3 mL of PIC solution (1 mg/mL) with a 0.45 μm Millipore filter (Durapore) into a clean scintillation vial. To determine the LCST, the temperature was raised at about 0.5 $^{\circ}C$ /min from 25 to 50 $^{\circ}C$ with steps of 1 or 3 $^{\circ}C$ depending on the proximity of the LCST. The solution was allowed to equilibrate until a stable reading of the intensity was obtained. Experiment duration was in the range of 5–20 min, and each experiment was repeated two or more times. Monomodal cumulants analysis or CONTIN were used to fit the data. Measurements as a function of the ionic strength were performed at 15 and 50 $^{\circ}C$ by adding the proper amount of 2 M NaCl to the PIC solution (1 mg/mL).

Static Light Scattering (SLS). PIC solutions in NaCl 0.001 M with concentrations ranging from 0.2 to 1.0 mg/mL were prepared and filtered as described in DLS. Data were elaborated by a Zimm plot to obtain weight-average molecular weight (M_w), z -average radius of gyration (R_g) and second virial coefficient (A_2).

Scanning Electron Microscopy (SEM). Scanning electron microscopy (SEM) images were obtained by using a LEO 1450 VP electron microscope. Samples were prepared by depositing a

droplet of 0.001 M NaCl aqueous solution of PIC (0.1 mg/mL) onto a freshly prepared mica surface and drying at room temperature.

Energy Filtered-Transmission Electron Microscopy (EF-TEM). The samples were observed in a Zeiss EM902 transmission electron microscope (TEM), operating at 80 kV and equipped with an “in-column” electron energy filter. The filter was settled to collect only elastic electrons ($\Delta E = 0$), with the result to enhance image contrast and resolution due to the elimination of the inelastic electrons in the image formation (reduction of the chromatic aberration). Samples were negative stained by a 2% w/v solution of phosphotungstic acid (PTA) buffered at pH = 7.3. Briefly, a droplet of a 0.001 M NaCl solution of the PIC micelles (1 mg/mL) was deposited onto 400 mesh copper grids covered with a very thin (about 20 nm) amorphous carbon film. The excess of liquid was removed by placing the grid onto a piece of filter paper. Finally, the grid was dried at room temperature, stained adding a droplet of the stain solution removing the excess by filter paper.

Results and Discussion

Synthesis of Diblock Copolymers. The structures of the block copolymers used in this study are reported in Scheme 1. We have already reported synthesis and association properties in aqueous solution of PAMPS-*b*-PNIPAAm block copolymers.³⁴ In this research three block copolymers named PAMPS₃₆-*b*-PNIPAAm₉₆, PAMPS₉₈-*b*-PNIPAAm₉₄, and PAMPS₉₈-*b*-PNIPAAm₄₀ will be used, with the subscript indicating the number-average degree of polymerization of the block. Their molecular weight and polydispersity data are reported elsewhere.³⁴

PEO-*b*-PAMPTMA block copolymers have been synthesized using a PEO macroinitiator prepared by esterification of the terminal hydroxyl group of poly(ethylene oxide) methyl ether (PEO-OH) with 2-bromopropionyl bromide. Two macroinitiators starting from PEO₄₅-OH and PEO₁₁₄-OH were prepared. ¹H NMR spectra demonstrated that complete esterification of terminal OH was obtained (data not reported). The ATRP of AMPTMA using PEO-Br macroinitiators was carried out using the conditions already reported by our group for ATRP of PAMPTMA.³⁶ The polymerization was controlled showing a linear first-order kinetic plot up to high conversions indicating that the concentration of active species remains constant during the polymerization (Figure 1a). A significant increase in the molecular weight was observed by GPC measurements, indicating the formation of the block copolymer. In Figure 1b, the values of M_n and M_w/M_n obtained by GPC are reported as a function of the conversion of AMPTMA. The number-average molecular weight increased linearly with conversion and the values were in reasonable agreement with the theoretical values calculated on the basis of conversion measured by HPLC (Table 1). M_w/M_n was reasonably low during the course of the polymerization and reached

values of 1.14–1.18 at high conversion, confirming the control of the polymerization. ^1H NMR spectrum of PEO-*b*-PAMPTMA is reported in Figure 2. The signals observed in the range of 1.5–2.0 ppm were assigned to the main chain protons (*l*, *m*) and to the central ethylene of propyl group (*o*) of PAMPTMA. The signals in the range of 3.0–3.5 ppm were attributed to the *n* and *p* protons of the methylenes of the propyl group of PAMPTMA and to the *q* protons of the methyl groups of PAMPTMA. The signal of PEO (*i*) was at about 3.6 ppm. The ratio of number-average degree of polymerization ($X_{n,\text{NMR}}$) of PEO and PAMPTMA was determined from the integral ratio of the signals due to the methyl and methylene protons in the side chain of the PAMPTMA block (*n*, *p*, and *q*) and the PEG protons (*i*). The values listed in Table 1 were in good agreement with the theoretical values calculated by HPLC. Three block copolymers were prepared and will be named PEO₄₅-*b*-PAMPTMA₁₀₀, PEO₁₁₄-*b*-PAMPTMA₁₀₀, and PEO₁₁₄-*b*-PAMPTMA₅₀.

Preparation of Polyion Complex Micelles. In the following discussion, the block copolymers PAMPS_{*x*}-*b*-PNIPAAm_{*y*} and PEO_{*n*}-*b*-PAMPTMA_{*m*} will be further abbreviated as A_{*x*}N_{*y*} and E_{*n*}A_{*m*}, respectively. PIC micelles were prepared by mixing the proper amount of block copolymers in order to obtain a 1 mg/mL PIC solution in 0.001 M NaCl as described in the Experimental Section. The block copolymers were mixed to obtain complete charge neutralization (mole fraction of positively charged unit, $f^+ = 0.5$) because it was demonstrated that this leads to the formation of PIC micelles

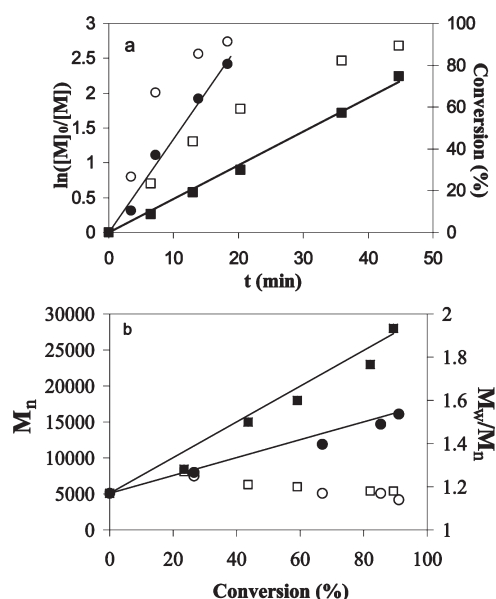


Figure 1. (a) First order kinetic plot (filled symbols) and conversion (open symbols) for ATRP of AMPTMA with PEO₁₁₄-Br macroinitiator in DMF:H₂O 50:50 (v/v) at 20 °C. [AMPTMA]₀ = 1.25, [PEO₁₁₄-Br]:[CuCl]:[Me₆TREN] = 1:1:1. Key: (●) [AMPTMA]:[PEO₁₁₄-Br] = 60:1; (■) [AMPTMA]:[PEO₁₁₄-Br] = 120:1. (b) Evolution of molecular weight (filled symbols) and polydispersity (open symbols) with conversion. The straight line represents the theoretical molecular weights expected on the basis of conversion measured by HPLC.

with maximum aggregation numbers and better defined size and morphology.^{1,9,11} Furthermore, since significant chain length recognition has been observed in PIC micelle formation,^{1,9,11} block copolymers with similar chain length of charged segments were mixed. In this way, four different PIC micelles were prepared, A₃₆N₉₆/E₁₁₄A₅₀, A₉₈N₄₀/E₄₅A₁₀₀, A₉₈N₄₀/E₁₁₄A₁₀₀, and A₉₈N₉₄/E₁₁₄A₁₀₀. After mixing of the block copolymers slightly turbid solutions were obtained. These solutions were stable for at least one month during which no precipitation was observed.

Proton Nuclear Magnetic Resonance. ^1H NMR spectrum of A₃₆N₉₆/E₁₁₄A₅₀ PIC micelles in a 0.001 M NaCl D₂O solution, C_p = 10 mg/mL at 25 °C are reported in Figure 2c. Significant decrease of the signals due to PAMPS and PAMPTMA blocks was observed with respect to those associated with the PEO and PNIPAAm blocks. This observation suggests that PIC micelles with a interpolyelectrolyte core were formed and both PEO and PNIPAAm blocks form a shell that stabilize the nanoparticles in aqueous solution, inducing a remarkable decrease of the mobility of PAMPS and PAMPTMA chains. The presence of residual signals of the polyion blocks could be due to the formation of a not very compact core with the presence of a significant amount of water. This aspect will be discussed again later.

^1H NMR experiments were also used to monitor the collapse of the PNIPAAm chains by increasing the temperature. As can be seen in Figure 2d, PNIPAAm signals disappeared upon collapse and formation of a hydrophobic

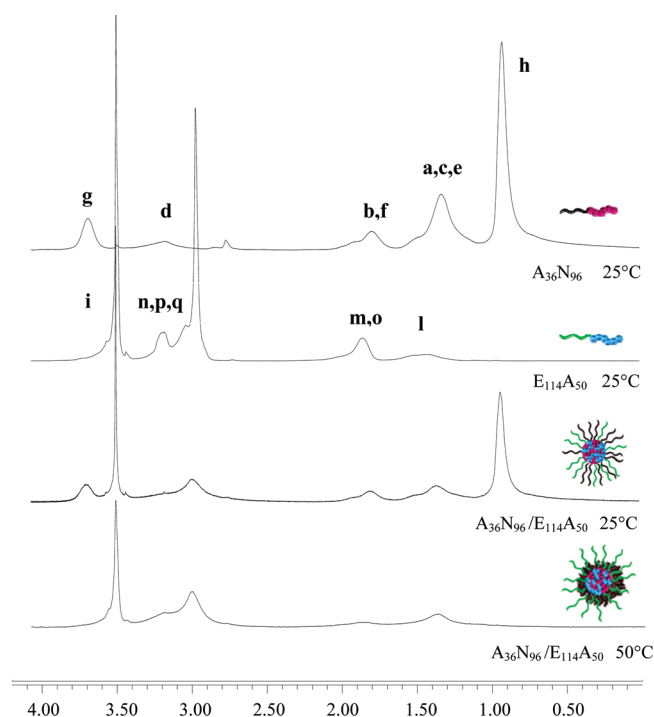


Figure 2. ^1H NMR spectra measured at C_p = 1.0 mg/mL in 0.001 M NaCl D₂O for (a) PAMPS₃₆-*b*-PNIPAAm₉₆ (A₃₆N₉₆), (b) PEO₁₁₄-*b*-PAMPTMA₅₀ (E₁₁₄A₅₀), (c) PIC micelles A₃₆N₉₆/E₁₁₄A₅₀ at 25 °C, and (d) PIC micelles A₃₆N₉₆/E₁₁₄A₅₀ at 50 °C.

Table 1. Number-Average Molecular Weight (*M_n*) and Molecular Weight Distribution (*M_w*/*M_n*) of PEO-*b*-PAMPTMA Copolymers

samples	<i>M_n</i> (theor) ^a	<i>M_n</i> (GPC)	<i>M_w</i> / <i>M_n</i> (GPC)	$\frac{X_{n,\text{PEO}}}{X_{n,\text{PAMPTMA}}}$ (theor) ^a	$\frac{X_{n,\text{PEO}}}{X_{n,\text{PAMPTMA}}}$ (NMR)
PEO ₄₅ - <i>b</i> -PAMPTMA ₁₀₀	20 200	23 200	1.16	0.45	0.44
PEO ₁₁₄ - <i>b</i> -PAMPTMA ₁₀₀	25 500	26 700	1.18	1.14	1.09
PEO ₁₁₄ - <i>b</i> -PAMPTMA ₅₀	14 400	16 100	1.14	2.28	2.10

^a Calculated from the monomer conversion obtained by HPLC.

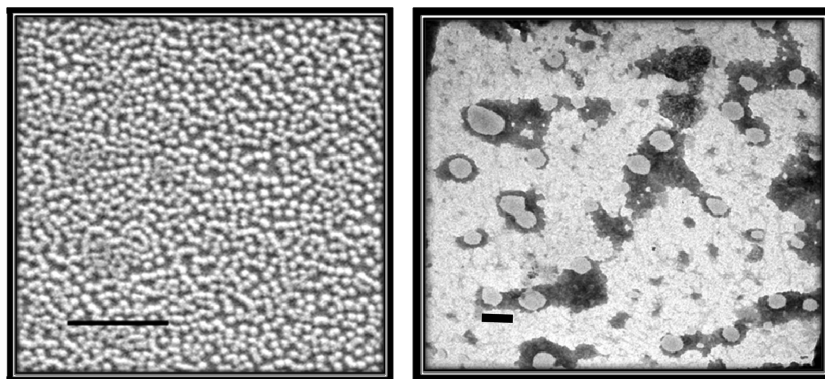


Figure 3. SEM (a) and TEM (b) images of PIC micelles $A_{36}N_{96}/E_{114}A_{50}$. Scale bar is 1 μm (SEM) and 100 nm (TEM).

Table 2. Association Properties of PIC Micelles Obtained by DLS and SLS in NaCl 0.001 M^a

sample	LCST ($^{\circ}\text{C}$)	R_h^b (nm)	R_g (nm)	R_g/R_h	M_w (10^7)	N_{agg}	A_2 (mol mL/g ²)	dn/dc_p (mL/g)
$A_{36}N_{96}/E_{114}A_{50}$	34	42.4	54.3	1.28	0.70	368	4.83×10^{-6}	0.216
$A_{98}N_{40}/E_{114}A_{100}$	37	43.8	51.3	1.33	1.33	503	6.45×10^{-7}	0.225
$A_{98}N_{40}/E_{45}A_{100}$	37	47.6	61.4	1.29	1.73	693	-4.29×10^{-6}	0.243
$A_{98}N_{94}/E_{114}A_{100}$	34	52.1	64.6	1.24	1.18	400	3.77×10^{-6}	0.248

^a $T = 20^{\circ}\text{C}$. DLS measurements were carried out at $C_p = 1$ mg/mL. ^b Obtained by cumulants analysis.

domain due to the loss of mobility resulting in significant peak broadening. This also means that the presence of PEO chains does not interfere with the formation of hydrophobic PNIPAAm domain. At the same time, PNIPAAm does not considerably affect the mobility of PEO chains because the intensity of PEO signals remains essentially the same. All proton signals were recovered upon cooling to room temperature, indicating the thermal transition is completely reversible.

Scanning and Transmission Electron Microscopy. Direct visualization of PIC micelles was obtained by scanning and transmission electron microscopy. Sample preparation and staining were made at room temperature. Representative micrographs are reported in Figure 3. Both techniques demonstrate the formation of spherical particles almost monodisperse in size, with diameter in the range of 50–100 nm. The particles are not aggregated, indicative of good stabilization of the interpolyelectrolyte core due to the PEO and PNIPAAm chains of the shell.

Dynamic Light Scattering (DLS). *Micellar Characteristic at Room Temperature.* There was a significant increase of the scattered intensity by mixing the block copolymers indicating the formation of larger aggregates. The relaxation rates (Γ) measured at different scattering angles plotted as a function of the square of the scattering vector (q^2) (see Supporting Information) gave a straight line passing through the origin, which means that the relaxation modes are virtually diffusive and the PIC micelles are spherical in shape and not much polydisperse in size.³⁷ Thus, the apparent hydrodynamic diameter (D_h) determined at a fixed angle of 90° was calculated by the Stokes–Einstein equation. Furthermore, D_h was independent of polymer concentration (C_p) from 0.2 to 1.0 mg/mL, suggesting the absence of secondary aggregates in the measured concentration region. Hence, D_h was measured at $C_p = 1$ mg/mL.

D_h distributions measured by intensity obtained by CONTIN analysis were all unimodal and narrow, with low polydispersity. R_h values are listed in Table 2. The size measured by DLS were in good agreement with the results obtained by TEM. The values are similar to that obtained by Shi et al. for PNIPAM₉₃-*b*-P4VP₅₈/PEG₁₁₄-*b*-P4VP₅₈ and PtBA₄₅-*b*-PNIPAAm₉₁/PtBA₆₀-*b*-P4VP₈₀ mixed micelles

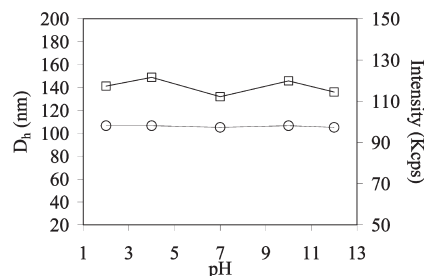


Figure 4. Dependence of the scattered intensity (\square) and D_h (\circ) on pH for $A_{98}N_{94}/E_{114}A_{100}$ PIC micelles obtained by DLS in 0.001 M NaCl aqueous solutions, with $C_p = 1$ mg/mL. The scattering angle was 90° . D_h was obtained by cumulants analysis.

with a mixed PNIPAAm shell,^{32,33} by Yusa et al. for PIC micelles formed PAMPS₁₀₈-*b*-PEO₄₇/PMAPTAC₁₀₆-*b*-PEO₄₇¹ and by He et al. for PIC micelles obtained mixing PEO–PNIPAAm–PLys star terpolymers with PAA.¹² Instead, the size is bigger than that obtained for PEO-*b*-PAsp/PEO-*b*-PLys PIC micelles with comparable block lengths.¹¹ These solutions were stable for at least one month during which no significant change of the size of the nanoparticles was observed. Furthermore, the PIC micelles isolated by lyophilization and redissolved in distilled water showed the same size.

Effect of pH. Because of the presence of two strong polyelectrolyte segments in the diblock copolymers, pH should not influence the existence of the PIC micelles. The dependence of the scattered intensity and D_h on pH for $A_{98}N_{94}/E_{114}A_{100}$ PIC micelles is reported in Figure 4. As expected, the data confirmed that micelles stability does not depend on pH on a wide range of pH.

Micellar Characteristic above LCST. By increasing the temperature it can be assumed, in a first approximation, that PNIPAAm chains in the PIC shell collapse forming an hydrophobic shell around the interpolyelectrolyte core transforming the core–shell PIC micelles in a core–shell–corona structure (Figure 6a).^{32,33} We will discuss this hypothesis again later. The increase of the scattered intensity as a function of the temperature measured at a fixed angle of 90° was used to determine the LCST of PNIPAAm chains located in the shell

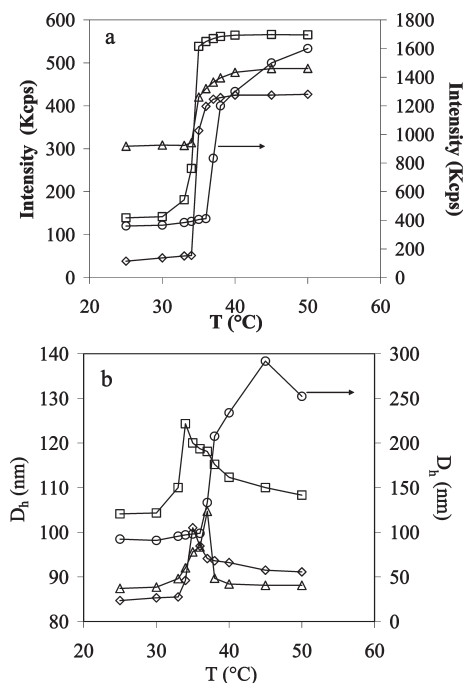


Figure 5. Temperature dependence of the scattered intensity (a) and D_h (b) obtained by DLS of PIC micelles in 0.001 M NaCl aqueous solutions, with $C_p = 1$ mg/mL. The scattering angle was 90° . D_h was obtained by cumulants analysis. Key: (\triangle) $A_{98}N_{40}/E_{114}A_{100}$, (\diamond) $A_{36}N_{96}/E_{114}A_{50}$, (\square) $A_{98}N_{94}/E_{114}A_{100}$, and (\circ) $A_{98}N_{40}/E_{45}A_{100}$. Values of $A_{98}N_{40}/E_{45}A_{100}$ have to be read on the secondary axis.

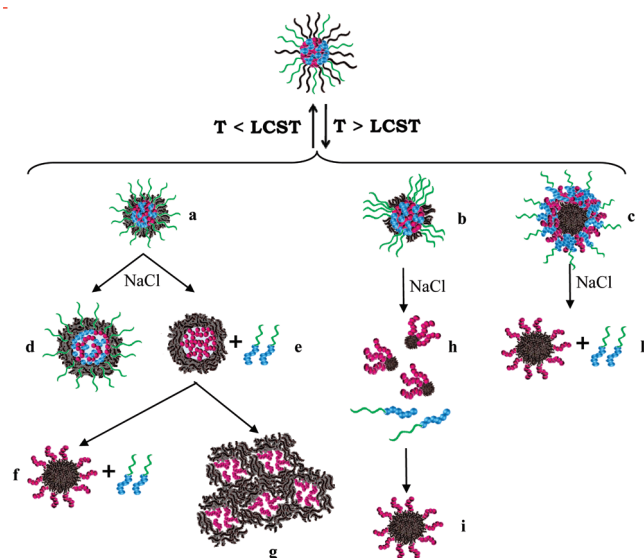


Figure 6. Schematic illustration of the possible mechanism involved in the formation, temperature dependence, and ionic strength dependence of PIC micelles.

(Figure 5a). LCSTs were determined as the intersection of the straight line passing through the inflection point of the curve and the horizontal straight line passing through the points before the transition and are listed in Table 2. LCSTs were obtained ranging between 34 and 37 °C and depending mainly on the PNIPAAm molecular weight.^{34,38} These values are 1–2 °C lower than those obtained for PAMPS-*b*-PNIPAAm thermo-induced micellization.³⁴

The increase of scattered intensity could be due to a change of refractive index or size of the particles. Figure 5b shows

the temperature dependence of the hydrodynamic diameter of PIC micelles. A similar behavior was observed for all the samples except for $A_{98}N_{40}/E_{45}A_{100}$. D_h increased with temperature reaching a maximum at around the LCST of PNIPAAm, then decreased to a plateau value. The final D_h is quite similar to that measured before the thermal transition, a maximum of about 5 nm increase was observed, which means that PEO chains effectively shield the PNIPAAm hydrophobic shell avoiding intermicellar interactions and aggregates formation. This behavior has been already observed by other authors,^{32,33} while Voets et al. observed significant aggregation upon heating a P2MVP₃₈-*b*-PEO₂₁₁/PAA₅₅-*b*-PNIPAAm₈₈ PIC micelles.¹⁰ The absence of aggregation at high temperature indicates that the PIC micelles of our study are not Janus micelles.³² It is worth mentioning that only the size of $A_{98}N_{40}/E_{114}A_{100}$ micelles at the end of the thermal transition was exactly the same as below LCST. This was reasonable considering that this PIC has the longest PEO chains and the shortest PNIPAAm chains. The temporary increase of D_h around LCST could be due to intermicellar interactions between PNIPAAm chains in the course of the transition when they have not yet completely collapsed close to the micellar core and are partly exposed near the PEO corona-solvent boundary. A different behavior was observed for $A_{98}N_{40}/E_{45}A_{100}$. In this case D_h showed a significant increase from 95 to 260 nm. It is reasonable that the short PEO chains of this PIC are not able to effectively screen the hydrophobic PNIPAAm shell and intermicellar aggregation takes place. No hysteresis has been observed for the temperature dependence of D_h and scattering intensity. More or less the same values of D_h and scattering intensity were observed when the temperature was decreased again to room temperature after the thermal transition.

Effect of Addition of Salt below LCST. It is important to evaluate the effect of the addition of NaCl on the stability of PIC micelles both below and above LCST. The experiments below LCST were carried out at 15 °C instead of 25 °C because the increase of ionic strength could induce a decrease of LCST of PNIPAAm below room temperature.³⁹ The ionic strength dependence of the scattered intensity and D_h at 15 °C are reported in Figure 7. After an initial range of ionic strength in which the scattered intensity and D_h remained constant, there was an increase up to a maximum value, after which both decreased reaching a plateau. The final values of D_h were all more or less coincident with the values of the block copolymers unimers, which indicate that at high ionic strength electrostatic interactions between the charged segments of the block copolymers were completely shielded and PIC micelles were disassembled. The intermediate maximum of D_h could be due to partial screening of the electrostatic interactions which become weaker giving rise to the swelling of the interpolyelectrolyte core and, eventually, to a temporary increase of PIC size. The ionic strength at which the maximum of D_h and the disassembling of the PIC micelles were observed depend mainly on the length of the charged segments but also on the length of the PEO and PNIPAAm blocks. $A_{36}N_{96}/E_{114}A_{50}$ PIC micelles, having the shortest polyion blocks, disassembled at the lowest ionic strength. An intermediate stability was observed for $A_{98}N_{40}/E_{45}A_{100}$ which has short PEO chains in the shell. The more stable PICs were $A_{98}N_{40}/E_{114}A_{100}$ and $A_{98}N_{94}/E_{114}A_{100}$, which have the longest polyion and PEO chains.

Effect of Addition of Salt Above LCST. $A_{98}N_{40}/E_{45}A_{100}$ was not studied because of the formation of large aggregates above LCST. A very different behavior was observed by increasing NaCl concentration at 50 °C, above the LCST of

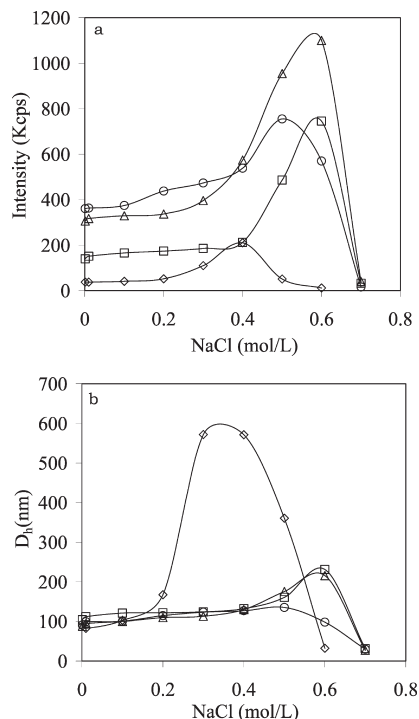


Figure 7. Ionic strength dependence of the normalized scattered intensity (a) and D_h (b) of PIC micelles obtained by DLS. $C_p = 1$ mg/mL, $T = 15$ °C, scattering angle was 90°. D_h was obtained by cumulants analysis. Key: (\triangle) $A_{98}N_{40}/E_{114}A_{100}$, (\diamond) $A_{36}N_{96}/E_{114}A_{50}$, (\square) $A_{98}N_{94}/E_{114}A_{100}$, and (\circ) $A_{98}N_{40}/E_{45}A_{100}$.

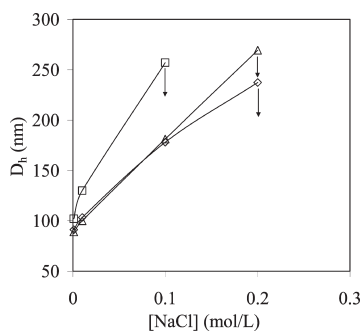


Figure 8. Ionic strength dependence of D_h of PIC micelles at 50 °C obtained by DLS. $C_p = 1$ mg/mL, scattering angle 90°. D_h was obtained by cumulants analysis. The last point of each curve corresponds to the highest NaCl concentration at which evident precipitation was not observed. Key: (\triangle) $A_{98}N_{40}/E_{114}A_{100}$, (\diamond) $A_{36}N_{96}/E_{114}A_{50}$, and (\square) $A_{98}N_{94}/E_{114}A_{100}$.

PNIPAAm (data not reported). A strong increase of turbidity and of scattered intensity was observed starting at 0.1 M NaCl, followed by precipitation between 0.2 and 0.4 M NaCl. D_h initially increase as expected for a progressive swelling of the coacervate core upon screening of interpolyelectrolyte interactions. Above about 0.2 M NaCl D_h could not be determined due to excess of scattering and precipitation (Figure 8). This behavior will be discussed in the following section.

Changes in Micellar Structure upon Temperature and Salt Concentration Increase. To explain these results, the mechanism involved in the thermal transition of PNIPAAm and the subsequent effect of ionic strength have to be examined in more detail also considering the models already proposed by other authors for mixed micelles having a PNIPAAm mixed shell.^{10,12,32,33} Several hypotheses can be formulated as

reported in Figure 6. A dramatic rearrangement of the micellar core might take place after thermal transition (Figure 6c), forming nanoparticles with PNIPAAm collapsed in a hydrophobic compact inner core covered by an interpolyelectrolyte layer, which in turn is surrounded and stabilized by PEO chains.¹⁰ Core-shell-corona type micelles should be formed in this hypothesis. Addition of salt would disrupt the coacervate shell of PIC micelles and dissolution of PEO-*b*-PAMPTMA should take place. Smaller micelles with a PNIPAAm core and PAMPS corona should be formed (Figure 6l). Precipitation observed upon addition of salt allowed us to exclude this hypothesis.

Otherwise, without this dramatic core rearrangement, PNIPAAm collapse could give rise to the formation of a hydrophobic PNIPAAm shell around the coacervate core with PEO corona stabilizing the nanoparticles (Figure 6, parts a and b).^{10,12,32,33} Depending on the relative amount of PEO and PNIPAAm, two different situations could be observed. First, if the amount of PNIPAAm is low, separately distributed, not interconnected PNIPAAm domains around the coacervate core may be formed, with large domains of freely moving and solvated PEO chains separating them (Figure 6b).³² This situation corresponds to that of "patched" micelles.^{40,41} Second, if the amount of PNIPAAm is high, continuous PNIPAAm shell may be formed with interconnected PNIPAAm domains. The nanoparticles are stabilized by PEO chains penetrating the PNIPAAm layer through small channels in which reasonably they retains a certain degree of hydration and mobility (Figure 6a).³² In the first case, NaCl addition should induce a decrease of D_h due to disassembling of PIC micelles followed by an increase of D_h due to the aggregation of the small PAMPS-*b*-PNIPAAm nanoparticles into large compound micelles.³² Also in this hypothesis, precipitation should not take place. In the other case, the continuous PNIPAAm shell should not be disassembled upon NaCl addition. If PEO-*b*-PAMPTMA does not leave the nanoparticles, these will continue to be stabilized and only on increase of size due to the core swelling should take place (Figure 6d).³² Otherwise, after an initial increase of size due to swelling of the coacervate core, the PEO-*b*-PAMPTMA chains could leave the PIC micelles and the PNIPAAm hydrophobic shell will no more be screened. If the system is not able to rearrange creating a PNIPAAm core surrounded by PAMPS chains (Figure 6f), precipitation should take place (Figure 6g). This is the only hypothesis explaining our experimental results.

To confirm this hypothesis we made a GPC measurement on the solution obtained by eliminating the precipitate described above by filtration (0.1 μ m) at 50 °C. The presence of an amount of PEO-*b*-PAMPTMA comparable to that used to prepare the PIC micelles confirmed that this polymer was released after NaCl addition at 50 °C, otherwise it would have been eliminated with the precipitate during filtration.

We think that is reasonable that the channels in the PNIPAAm shell through which PEO chains pass toward the outer part of the PIC micelle and that allowed the uptake of water and NaCl, will also allow the PAMPTMA chains to go through.

It could also be possible that, by adding NaCl, decrease of electrostatic repulsion between polyelectrolytes and increase of hydrophobic or van der Waals attraction between all the polymers could lead to aggregation and consequently precipitation of PIC micelles. We can exclude this hypothesis because we have unpublished data on the shell-cross-linking of thermally formed micelles of PAMPS-*b*-PNIPAAm with PEO-*b*-PAMPTMA showing that there was no precipitation by adding NaCl at temperature above LCST. The simple

Table 3. Core Radius (R_c), Shell Radius (R_s), Contour length (L), Polymer Density at Core-Shell Interface (Φ), Volume of Collapsed PNIPAAm Shell (V_{PNIPAAm}), and Volume of PEO Chains Inside the Collapsed PNIPAAm Shell (V_{PEO}) of PIC Micelles.^a

sample	R_c (nm)	R_s (nm)	L_{PEO} (nm) ^b	L_{PNIPAAm} (nm) ^b	$\Phi_{25\text{ }^\circ\text{C}}$ (chain/nm ²)	$\Delta R_{\text{PNIPAAm}}$ (nm)	V_{PNIPAAm} (nm ³)	W_{PEO}	V_{PEO} (nm ³)	$\Phi_{50\text{ }^\circ\text{C}}$ (chain/nm ²)
A ₃₆ N ₉₆ /E ₁₁₄ A ₅₀	11.0	31.4	38.8	24	0.24	0.83	1.4×10^3	0.25	24	0.09
A ₉₈ N ₄₀ /E ₁₁₄ A ₁₀₀	16.3	27.5	38.8	10	0.15	1.22	4.3×10^3	0.53	58	0.06
A ₉₈ N ₄₀ /E ₄₅ A ₁₀₀	18.1	29.5	15.3	10	0.17	1.36	6.0×10^3	0.32	89	0.07
A ₉₈ N ₉₄ /E ₁₁₄ A ₁₀₀	15.1	37.0	38.8	23.3	0.14	1.13	3.5×10^3	0.31	43	0.06

^a NaCl 0.001 M. $T = 25\text{ }^\circ\text{C}$ if not stated otherwise. ^b Contour length of the repeating unit is 0.25 and 0.34 nm for PNIPAAm and PEO, respectively.

dissociation of PEO-*b*-PAMPTMA from PAMPS-*b*-PNIPAAm micelles was observed. In our opinion this confirms that at $T > \text{LCST}$ and high NaCl concentration, hydrophobic or van der Waals attraction between the polymers did not become significant.

Concerning the formation of an interconnected PNIPAAm hydrophobic shell Shi et al.³² found that, for complex micelles with a P4VP core surrounded by a mixed PNIPAAm/PEG shell, the weight fraction of PEO (W_{PEO}) in the mixed PEO/PNIPAAm shell at $25\text{ }^\circ\text{C}$ is an important factor. They found that a continuous PNIPAAm hydrophobic shell was formed above LCST if $W_{\text{PEO}} = 0.41$ while separately distributed PNIPAAm domains were formed if $W_{\text{PEO}} = 0.58$. Our PIC micelles have W_{PEO} in the range from 0.25 to 0.53 (Table 3), which suggests the formation of a continuous PNIPAAm hydrophobic shell (Figure 6a) for all the PIC micelles with the only doubt of A₉₈N₄₀/E₁₁₄A₁₀₀. This argument will be further considered later discussing SLS measurements.

Static Light Scattering (SLS). There was no sign of a change in the size of PIC micelles with concentration in the measured range from 0.01 to 1 mg/mL, suggesting that PIC micelles studied here are stable upon dilution, and have no critical association concentration (cac) at least in the range higher than 0.01 mg/mL. Hence, the apparent values of M_w , R_g , and A_2 for PIC micelles were determined by SLS by Zimm plots (see Supporting Information) in the concentration range of 0.2–1 mg/mL (Table 2).

The values of A_2 were all positive except for the A₉₈N₄₀/E₄₅A₁₀₀ PIC micelles that had a negative A_2 . This means that 0.001 M NaCl is not a good solvent for this PIC confirming, as observed by DLS measurements below and above LCST, that short PNIPAAm and PEO chains does not effectively screen the interpolyelectrolyte core.

R_g values were used to calculate R_g/R_h which is well-known to reveal the morphology of particles in solution.^{42–47} The R_g/R_h ratio for a solid sphere is 0.774⁴⁷ while for random coils of homopolymers is about 1.50.⁴³ Thus, the values obtained (Table 2) could be indicative of core-shell micelles with highly extended and hydrated shell chains and/or with a not very compact coacervate core.¹² The second hypothesis seems to be confirmed by the presence of residual polyelectrolyte signals in the ¹H NMR spectra of PIC micelles (Figure 2) and by the values of R_h that are not much smaller than the values of the contour length L of the fully extended block copolymer chains. The conformation of the chains in the PIC shell will be discussed again later with the data of the shell density.

The aggregation number (N_{agg}), defined as the total number of polymer chains forming one PIC micelle, is given by

$$N_{\text{agg}} = N_{\text{EA}} + N_{\text{AN}} \quad (1)$$

where N_{EA} and N_{AN} are the number of PEO-*b*-PAMPTMA and PAMPS-*b*-PNIPAAm chains in the PIC micelle, respectively.

N_{EA} and N_{AN} can be calculated by the equations

$$N_{\text{EA}} = N_{\text{agg}} \frac{X_{\text{n, PAMPS}}}{X_{\text{n, PAMPS}} + X_{\text{n, PAMPTMA}}},$$

$$N_{\text{AN}} = N_{\text{agg}} \frac{X_{\text{n, PAMPTMA}}}{X_{\text{n, PAMPS}} + X_{\text{n, PAMPTMA}}} \quad (2)$$

where $X_{\text{n, PAMPS}}$ and $X_{\text{n, PAMPTMA}}$ are the number-average degree of polymerization of the charged blocks. The equations of N_{EA} and N_{AN} take into account the prerequisite of charge stoichiometric balance of the PIC micelles. For almost monodisperse micelles formed by block copolymers with low polydispersity, M_w measured by SLS can be written in a first approximation as

$$M_{w, \text{PIC}} = N_{\text{EA}} M_{\text{n, EA}} + N_{\text{AN}} M_{\text{n, AN}} \quad (3)$$

where $M_{\text{n, EA}}$ and $M_{\text{n, AN}}$ are the number-average molecular weights of the charged blocks.

The values of N_{agg} , calculated by introducing eqs 2 in eq 3 and rearranging, are listed in Table 2. Values from about 368 to 693 were obtained. There was not a significant influence of the block length on the formation of the PIC micelles if compared with the results obtained by other authors for chain length matching PAMPS-*b*-PEO/PMAPTAC-*b*-PEO PIC micelles formed by polyion segments of 28 and 108 repeating units.¹

Likewise to what established for micelles formed by amphiphilic block copolymers, N_{agg} should depend on the length of the two blocks, $N_{\text{agg}} = N_c^\alpha N_s^{-\beta}$, where N_c and N_s are the number-average degree of polymerization of the core and shell forming blocks, respectively.^{48–50} Hence N_{agg} increases with increasing the size of the core forming blocks and decreasing the size of the shell forming block. Indeed, the lower value was obtained for the A₃₆N₉₆/E₁₁₄A₅₀ PIC micelles containing the shortest polyelectrolyte chains and the longest PEO and PNIPAAm chains. By using the longest polyelectrolyte chains, N_{agg} increased as the length of PEO and PNIPAAm chains decreased. It has to be underlined that the values of N_{agg} could also be influenced by intermicellar aggregation that, as already mentioned before, could take place for A₉₈N₄₀/E₄₅A₁₀₀.

The core radius (R_c) of the PIC micelles was calculated by the equation

$$R_c = \left[\frac{3}{4} \pi V_c \right]^{1/3} = \left[\frac{3}{4 \pi N_A} \left(\frac{N_{\text{AN}} M_{\text{n, PAMPS}}}{\rho_{\text{PAMPS}}} + \frac{N_{\text{EA}} M_{\text{n, PAMPTMA}}}{\rho_{\text{PAMPTMA}}} \right) \right]^{1/3} \quad (4)$$

where V_c is the volume of the single PIC micelle core, N_A is the Avogadro constant, and ρ_{PAMPTMA} and ρ_{PAMPS} are the

densities of the charged polymers. In a first approximation, ρ_{PAMPTMA} and ρ_{PAMPS} have been considered equal to the bulk densities of the monomers, $\rho_{\text{AMPTMA}} = 1.11 \text{ g/cm}^3$ and $\rho_{\text{AMPS}} = 1.21 \text{ g/cm}^3$.¹ Thus, R_c values (Table 3) were in the range 11.0–18.1 nm and were always lower than the contour length of the polyelectrolyte chains involved in the formation of the coacervate core. Furthermore, R_c values depends mainly on the length of the charged chains.

The shell thickness (R_s) was calculated as $R_s = R_h - R_c$ (Table 3). These values can be compared with the values of the contour length of the PEO and PNIPAAm chains (L_{PEO} and L_{PNIPAAm}) forming the shell in their fully extended conformation. If core–shell micelles without intermicellar aggregation were formed, R_s should be lower than L_{PEO} and L_{PNIPAAm} . This is true for all the PIC micelles except for $A_{98}N_{40}/E_{45}A_{100}$ that means that probably in this case intermicellar aggregation takes place. This is reasonable since these are the PIC micelles having the shortest PEO chains. This suggests that aggregation by intermicellar electrostatic interactions between PIC cores is prevented by the presence of long PEO chains ($X_{n,\text{PEO}} = 114$) with a contour length of the fully extended chain (L_{PEO} , assuming a monomer contour length of 0.34 nm) of 38.8 nm (Table 3). This confirms the behavior observed for $A_{98}N_{40}/E_{45}A_{100}$ above LCST.

Furthermore, the total PEO and PNIPAAm surface density at core/shell interface (Φ) was determined from N_{agg} and R_c using the following equation:

$$\Phi = \frac{N_{\text{agg}}}{4\pi R_c^2} \quad (5)$$

The calculated Φ values at 25 °C ($\Phi_{25\text{ °C}}$) are summarized in Table 3. As already reported by other authors for PIC micelles formed PEO-*b*-poly(α,β -aspartic acid) (PEO-*b*-PAsp) with PEO-*b*-poly(L-lysine) (PEO-*b*-PLys),¹¹ $\Phi_{25\text{ °C}}$ values are mainly due to the length of the polyelectrolyte chains forming the coacervate core, that is $\Phi_{25\text{ °C}}$ decreased as X_n of the charged chains increase. We found $\Phi_{25\text{ °C}} = 0.24 \text{ chain/nm}^2$ for $A_{36}N_{96}/E_{114}A_{50}$ and $\Phi_{25} = 0.14\text{--}0.17 \text{ chain/nm}^2$ for PIC micelles formed with the block copolymers with longer charged chains. These values are similar to those reported by other authors^{11,51} and suggest that the PEO and PNIPAAm segment at the core/shell interface are highly hydrated.¹¹ This could contribute to the high values of R_g/R_h measured for PIC micelles if significant solvent draining in the outer part of the PIC micelles takes place.

SLS data at 25 °C were also used to determine the surface density of PEO chains at the core/shell interface at 50 °C with PNIPAAm collapsed to form the hydrophobic layer around the coacervate core (Figure 6a). The thickness of the collapsed PNIPAAm shell ($\Delta R_{\text{PNIPAAm}} = R_{\text{hs}} - R_c$, where R_{hs} is the outer radius of the PNIPAAm hollow sphere) was obtained considering that PNIPAAm forms a hollow sphere structure around the coacervate core with a volume that can be calculated by the equation

$$V_{\text{PNIPAAm}} = \frac{4\pi(R_{\text{hs}}^3 - R_c^3)}{3} = \frac{N_{\text{AN}}M_{n,\text{PNIPAAm}}}{N_A\rho_{\text{PNIPAAm}}} \quad (6)$$

where ρ_{PNIPAAm} is the density of the PNIPAAm core, which in a first approximation can be taken equal to the density of bulk amorphous PNIPAAm (1.070 g/mL).⁵² Surprisingly, the values of ΔR are very small, from 0.83 to 1.36 nm. The PEO surface density at core/shell interface at 50 °C ($\Phi_{50\text{ °C}}$) can now be calculated (Table 3). With respect to the surface density at 25 °C the values above LCST were more or less halved because the corona of the core–shell–corona

structure formed after PNIPAAm collapse is now formed only by PEO chains. The contribution to this effect of the increase of the radius due to the thickness of the PNIPAAm shell is negligible. The values of surface density at 50 °C indicate that the PEO chains in the corona have a very low density and become more hydrated after the thermal transition.

The thickness of the collapsed PNIPAAm shell can also be used to calculate the volume of PEO chains passing through it (V_{PEO}). This might be used as a parameter to confirm the hypothesis that an interconnected continuous PNIPAAm shell is formed (Figure 6a). Assuming that the PEO chains go through the PNIPAAm shell in a completely stretched conformation, we can write

$$V_{\text{PEO}} = \frac{v_{\text{EO}}N_{\text{EA}}\Delta R_{\text{PNIPAAm}}}{L_{\text{EO}}} \quad (7)$$

where $v_{\text{EO}} = 0.0646 \text{ nm}^3$ is the molecular volume of the repeating unit of PEO, that has been calculated as the ratio of the weight of the repeating unit (ratio of the repeating unit molecular weight to the Avogadro number) to the density of bulk amorphous PEO ($\rho_{\text{PEO}} = 1.13 \text{ g/mL}$).⁵³ The values are reported in Table 3 together with the values of V_{PNIPAAm} . The volume fraction of PEO chains inside the PNIPAAm shell is always lower than 2%, confirming that is reasonable to assume that PNIPAAm forms a fully interconnected shell around the coacervate core. In our opinion this parameter is more indicative of the ability of this kind of micelles to form a continuous shell after thermal transition with respect to the calculation of the weight fraction of PEO in the mixed PEO/PNIPAAm shell at 25 °C. It has to be underlined that this value has been calculated without considering the possible hydration of PEO chains passing through the PNIPAAm hydrophobic shell. Anyway, is reasonable that even in this case the volume fraction of PEO hydrated chains would remain low enough to assume the formation of a continuous PNIPAAm shell.

In conclusion, we have reported the ATRP synthesis of poly[(3-acrylamidopropyl)trimethylammonium chloride]-*block*-poly(ethylene oxide), PAMPTMA-*b*-PEO, block copolymers using a PEO macroinitiator prepared by esterification of the terminal hydroxyl group of poly(ethylene oxide) methyl ether with 2-bromopropionyl bromide. Block copolymers with different PAMPTMA and PEO length were used to form thermosensitive and pegylated PIC micelles in aqueous solution with oppositely charged poly(sodium 2-acrylamido-2-methylpropanesulfonate)-*block*-poly(*N*-isopropylacrylamide), PAMPS-*b*-PNIPAAm, block copolymers under stoichiometric charge neutralization conditions and polyelectrolyte chain length matching. The PIC micelles were characterized by ¹H NMR, static light scattering (SLS), dynamic light scattering (DLS), and transmission electron microscopy (TEM) techniques.

At room temperature, spherical PIC micelles, consisting of a mixed PAMPTMA/PAMPS coacervate core and a mixed PEO/PNIPAAm shell, were formed, with size of about 80–110 nm. The PIC micelles completely dissociated to unimers by increasing NaCl concentration above 0.4–0.6 M. PNIPAAm segments in the shell gave rise to temperature induced transition at 34–37 °C forming a hydrophobic shell around the coacervate core. This means that core–shell–corona type PIC micelles were formed, with a PEO corona which stabilizes the nanoparticles in aqueous solution. A fully interconnected and continuous collapsed PNIPAAm shell was formed with PEO chains forming channels across the PNIPAAm membrane which allowed for solvent and ion

exchange. The association properties of the PIC micelles were influenced by the length of the block segments. Longer polyelectrolyte chains gave rise to bigger micelles, more stable with respect to the ionic strength. PNIPAAm chain length allowed modulating the temperature of the thermal transition. Long PEO chains (114 repeating units) were necessary to effectively stabilize PIC micelles both below and above LCST of PNIPAAm. Micelle parameters (core radius, R_c , shell radius, R_s , thickness and volume, $\Delta R_{\text{PNIPAAm}}$ and V_{PNIPAAm} , of the collapsed PNIPAAm shell and surface density, Φ , of shell and corona chains before and after the thermal transition) were determined and discussed in terms of block copolymer structure.

Precipitation was observed by addition of salt at temperature above LCST because of the release of PEO-*b*-PAMPT-MA chains. A detailed model was suggested explaining the formation and the response to temperature and ionic strength of the PIC micelles. This is the first example of pegylated and thermosensitive PIC micelles having a coacervate core formed by two strong polyelectrolyte blocks with no pH dependence that could be useful if the stability of the nanoparticles have to be independent of this parameter.

Acknowledgment. This work has been carried out with the financial support of the University "La Sapienza" (Ateneo Funds).

Supporting Information Available: Figures showing the dependence of the relaxation rates, calibration of the RI detector, measurements of dn/dc , and Zimm plots for micelles and text discussing the measurement of the refractive index increment. This material is available free of charge via the Internet at <http://pubs.acs.org>.

References and Notes

- Yusa, S.; Yokoyama, Y.; Morishima, Y. *Macromolecules* **2009**, *42*, 376–383.
- Voets, I. K.; De Keizer, A.; Cohen Stuart, M. A.; Justynska, J.; Schlaad, H. *Macromolecules* **2007**, *40*, 2158–2164.
- Voets, I. K.; Fokking, R.; Hellweg, T.; King, S. M.; de Waard, P.; De Keizer, A.; Cohen Stuart, M. A. *Soft Matter* **2009**, *5*, 999–1005.
- Voets, I. K.; De Keizer, A.; de Waard, P.; Cohen Stuart, M. A. *Macromolecules* **2006**, *39*, 5952–5955.
- Hofs, B.; De Keizer, A.; Van der Burgh, S.; Leermakers, F. A. M.; Cohen Stuart, M. A.; Millard, P.-E.; Mueller, A. H. E. *Soft Matter* **2008**, *4*, 1473–1482.
- Voets, I. K.; Van der Burgh, S.; Farago, B.; Fokkink, R.; Kovacevic, D.; Hellweg, T.; De Keizer, A.; Cohen Stuart, M. A. *Macromolecules* **2007**, *40*, 8476–8482.
- Cohen Stuart, M. A.; Besseling, N. A. M.; Fokkink, R. G. *Langmuir* **1998**, *14*, 6846–6849.
- Voets, I. K.; de Keizer, A.; Cohen Stuart, M. A. *Adv. Colloid Interface Sci.* **2009**, *147–148*, 300–318.
- Harada, A.; Kataoka, K. *Science* **1999**, *283*, 65–67.
- Voets, I. K.; Moll, P. M.; Aqil, A.; Jerome, C.; Detrembleur, C.; de Waard, P.; de Keizer, A.; Cohen Stuart, M. A. *J. Phys. Chem. B* **2008**, *112*, 10833–10840.
- Harada, A.; Kataoka, K. *Macromolecules* **2003**, *36*, 4995–5001.
- Li, J.; He, W.-D.; He, N.; Han, S.-C.; Sun, X.-L.; Li, L.-Y.; Zhang, B.-Y. *J. Polym. Sci. Part A: Polym. Chem.* **2009**, *47*, 1450–1462.
- Harada, A.; Kataoka, K. *Macromolecules* **1995**, *28*, 5294–5299.
- Kakizawa, Y.; Kataoka, K. *Adv. Drug Deliv. Res.* **2002**, *54*, 203–222.
- Kataoka, K.; Togawa, H.; Harada, A.; Yagusi, K.; Matsumoto, T.; Katayose, S. *Macromolecules* **1996**, *29*, 8556–8557.
- Harada, A.; Kataoka, K. *Macromolecules* **1998**, *31*, 288–294.
- Harada, A.; Kataoka, K. *Langmuir* **1999**, *15*, 4208–4212.
- Cohen Stuart, M. A.; Hofs, B.; Voets, I. K.; de Keizer, A. *Curr. Opin. Colloid Interface Sci.* **2005**, *10* (1–2), 30–36.
- Colfen, H. *Macromol. Rapid Commun.* **2001**, *22*, 219–252.
- Voets, I. K.; de Keizer, A.; de Waard, P.; Frederik, P. M.; Bomans, P. H. H.; Schmalz, H.; Walther, A.; King, S. M.; Leermakers, F. A. M.; Cohen Stuart, M. A. *Angew. Chem., Int. Ed.* **2006**, *45* (40), 6673–6676.
- Amiji, M.; Park, K. *Biomaterials* **1992**, *13*, 682–692.
- Popat, K. C.; Desai, T. A. *Biosens. Bioelectron.* **2004**, *19*, 1037–1044.
- Malmsten, M.; Emoto, K.; Van, A. J. M. *J. Colloid Interface Sci.* **1998**, *202*, 507–517.
- Gotoh, Y.; Tsukada, M.; Minoura, N.; Imai, Y. *Biomaterials* **1997**, *18*, 267–271.
- Wang, P.; Tan, K. L.; Kang, E. T.; Neoh, K. G. *J. Mater. Chem.* **2001**, *11*, 2951–2957.
- Lopez, G. P.; Albers, M. W.; Schreiber, S. L.; Carroll, R.; Peralta, E.; Whitesides, G. M. *J. Am. Chem. Soc.* **1993**, *115*, 5877–5878.
- Zhang, M.; Desai, T.; Ferreri, M. *Biomaterials* **1998**, *19*, 953–960.
- Dong, W.-F.; Kishimura, A.; Anraku, Y.; Chuano, S.; Kataoka, K. *J. Am. Chem. Soc.* **2009**, *131* (11), 3804–3805.
- Blanazs, A.; Armes, S. P.; Ryan, A. J. *Macromol. Rapid Commun.* **2009**, *30*, 267–277.
- Heskins, M.; Guillet, J. E.; James, E. J. *Macromol. Sci., Chem.* **1968**, *2*, 1441–1455.
- Yoshida, R.; Uchida, K.; Kaneko, Y.; Sakai, K.; Kikuchi, A.; Sakurai, Y.; Okano, T. *Nature* **1995**, *374*, 240–242.
- Ma, R.; Wang, B.; Xu, Y.; An, Y.; Zhang, W.; Li, G.; Shi, L. *Macromol. Rapid Commun.* **2007**, *28*, 1062–1069.
- Li, G. Y.; Shi, L. Q.; Ma, R. J.; An, Y. L.; Huang, N. *Angew. Chem., Int. Ed.* **2006**, *45*, 4959–4962.
- Masci, G.; Diociaiuti, M.; Crescenzi, V. *J. Polym. Sci., Part A: Polym. Chem.* **2008**, *46*, 4830–4842.
- Xia, J.; Gainor, S. G.; Matyjaszewski, K. *Macromolecules* **1998**, *31*, 5958–5959.
- Patrizi, M. L.; Diociaiuti, M.; Capitani, D.; Masci, G. *Polymer* **2009**, *50*, 467–474.
- Xu, R.; Winnik, M. A.; Hallett, F. R.; Riess, G.; Croucher, M. D. *Macromolecules* **1991**, *24*, 87–93.
- Xia, Y.; Yin, X.; Burke, N. A. D.; Stolter, H. D. H. *Macromolecules* **2005**, *38*, 5937–5943.
- Bokias, G.; Staikos, G.; Iliopoulos, I. *Polymer* **2000**, *41*, 7399–7405.
- Hoppenbrouwers, E.; Li, Z.; Liu, G. J. *Macromolecules* **2003**, *36*, 876–881.
- Yan, X. H.; Liu, G. J.; Hu, J. W.; Willson, C. G. *Macromolecules* **2006**, *39*, 1906–1912.
- Burchard, W. *Adv. Polym. Sci.* **1983**, *48*, 1–124.
- Tu, Y.; Wan, X.; Zhang, D.; Zhou, Q.; Wu, C. *J. Am. Chem. Soc.* **2000**, *122*, 10201–10205.
- Wu, C.; Zuo, J.; Chu, B. *Macromolecules* **1989**, *22*, 633–639.
- Antonietti, M.; Heinz, S.; Schmidt, M. *Macromolecules* **1990**, *23*, 3796–3805.
- Antonietti, M.; Wremser, W.; Schmidt, M.; Rosenauer, C. *Macromolecules* **1994**, *27*, 3276–3281.
- Mallamace, F.; Micali, N. In *Low Angle Light Scattering and Its Applications In Light Scattering: Principles and Development*; Brown, W., Ed.; Clarendon Press: Oxford, U.K., 1996; p 381.
- Burguière, C.; Chassenieux, C.; Charleux, B. *Polymer* **2003**, *44*, 509–518.
- Khogaz, K.; Astafieva, I.; Eisenberg, A. *Macromolecules* **1995**, *28*, 7135–7147.
- Forster, S.; Zisenis, M.; Wenz, E.; Antonietti, M. *J. Chem. Phys.* **1996**, *104*, 9956–9970.
- Yusa, S.; Sugahara, M.; Endo, T.; Morishima, Y. *Langmuir* **2009**, *25*, 5258–5265.
- Shields, D. J.; Coover, H. W. *J. Polym. Sci.* **1959**, *39*, 532–533.
- Fuller, C. S. *Chem. Rev.* **1940**, *26*, 143–167.